

# Physical solutions of the Kitaev honeycomb model

Fabio L. Pedrocchi,<sup>1</sup> Stefano Chesi,<sup>1,2</sup> and Daniel Loss<sup>1</sup>

<sup>1</sup>*Department of Physics, University of Basel, Klingelbergstrasse 82, CH-4056 Basel, Switzerland*

<sup>2</sup>*Department of Physics, McGill University, Montreal, Quebec, Canada H3A 2T8*

We investigate the exact solution of the Kitaev honeycomb model and derive an explicit formula for the projector onto the physical subspace. We show that in general there is a fundamental difference between the exact solutions of the projected and unprojected models. We consider physically relevant quantities such as spin-spin correlations and vortex energies and show that their true value can be substantially different from the one calculated in the unprojected space. Our projection protocol makes it possible to numerically study large spin models, intractable by direct diagonalization, whenever Kitaev's exact mapping is applicable.

PACS numbers: 75.10.Jm, 71.10.Pm, 03.67.Lx, 05.30.Pr

*Introduction.* The Kitaev honeycomb model, with several variations, has attracted a lot of attention over the last years [1–15]. Many different interesting aspects of it have been studied in detail in the original work of Kitaev [1]. There, an exact method of solutions of the model based on the mapping to Majorana fermion operators is discussed. Further, the presence of an abelian and a non-abelian phase (in the presence of an external magnetic perturbation) was demonstrated. The Kitaev honeycomb model has a wide spectrum of physical applications, ranging from the description of strongly correlated materials [2] to the analytical study of critical quantum spin liquids [3]. It is also of central importance in the context of quantum information theory since its gapped phase provides a perturbative realization of the toric code [4]. Extensions of the honeycomb model have been lately proposed as promising candidates for the realization of a topological quantum memory [5, 6]. Although very challenging, its physical realization has become closer to reality thanks to recent proposals [7, 8].

In this Letter, we reexamine the mapping proposed by Kitaev [1] and derive an explicit representation of the projector onto the physical subspace. Our analysis shows that the mapping does not simply introduce a large degeneracy (from the gauge symmetry group), but half of the eigenstates and eigenvalues are unphysical. That unprojected and projected models have different physical properties was apparently overlooked in the original publication [1] and all subsequent literature. The numerical solution of the model in the extended space leads to unphysical results for all physically relevant quantities, like ground state and vortex energies, or spin-spin correlation functions, and finite-size corrections are far from being negligible for relatively large lattice sizes (of order of a thousand spins). The projection protocol presented in this Letter is consequently essential for the exact numerical study via Kitaev's exact mapping of large spin systems, otherwise inaccessible via direct diagonalization [9–11].

*Model and exact mapping.* The Kitaev honeycomb model is a quantum compass model [16] defined on an

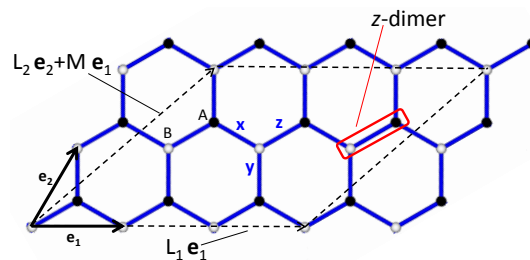


FIG. 1: Honeycomb lattice, with basis vectors  $\mathbf{e}_{1,2}$ . The directions of  $x, y, z$ -links are indicated, as well as A and B sublattices (white and black dots, respectively). The most general torus on the lattice can be specified by  $L_1 \mathbf{e}_1$  and  $L_2 \mathbf{e}_2 + M \mathbf{e}_1$  (here  $L_1 = 3$ ,  $L_2 = 2$ , and  $M = 1$ ).

hexagonal lattice  $\Lambda$  as follows

$$H = \sum_{\langle i,j \rangle} J_{\alpha_{ij}} \sigma_i^{\alpha_{ij}} \sigma_j^{\alpha_{ij}}, \quad (1)$$

where  $\sigma_i$  are the Pauli spin operators at site  $i \in \Lambda$  ( $i = 1, \dots, 2N$ ). In Eq. (1), the sum runs over all the pairs of nearest-neighbor sites and the directions of the Ising interactions are determined by the orientations of the corresponding links ( $\alpha_{ij} = x, y, z$  for  $x$ -,  $y$ -,  $z$ -links respectively, see Fig. 1).

To solve this spin model in an extended Hilbert space  $\tilde{\mathcal{L}}$ , one can associate at each site  $i$  four Majorana modes  $c_i, b_i^x, b_i^y, b_i^z$  [1]. By defining  $\tilde{\sigma}_i^\alpha = i b_i^\alpha c_i$ , the original Hamiltonian in Eq. (1) is mapped to

$$\tilde{H} = i \sum_{\langle i,j \rangle} \hat{A}_{ij} c_i c_j, \quad (2)$$

where for nearest-neighbor sites  $\hat{A}_{ij} = J_{\alpha_{ij}} \hat{u}_{ij}$  and

$$\hat{u}_{ij} = i b_i^{\alpha_{ij}} b_j^{\alpha_{ij}} = -\hat{u}_{ji}. \quad (3)$$

These operators satisfy  $\hat{u}_{ij}^2 = 1$ . Furthermore, they all commute with each other and also with  $\tilde{H}$ . Therefore, the extended Hilbert space splits into  $\tilde{\mathcal{L}} = \bigoplus_u \tilde{\mathcal{L}}_u$ , where  $u$  represents a configuration of  $u_{ij} = \pm 1$  [17]. In each

subspace  $\tilde{\mathcal{L}}_u$ , the operator matrix  $\hat{A}_{ij}$  are replaced by numbers  $A_{i,j}^u$  and Eq. (2) thus describes non-interacting Majorana fermions.

The eigenmodes can be easily obtained with a canonical transformation to new Majorana operators

$$(b'_1, b''_1, \dots, b'_N, b''_N) = (c_1, \dots, c_{2N})Q^u. \quad (4)$$

which for the specific configuration  $u$  brings  $\tilde{H}$  to the form  $\tilde{H}_u = \frac{i}{2} \sum_m \epsilon_m b'_m b''_m$ , where  $\epsilon_m$  are the positive eigenvalues of  $2iA^u$ . By introducing the fermion operators  $a_m = 1/2(b'_m - ib''_m)$  and  $n_m = a_m^\dagger a_m$  we obtain

$$\tilde{H}_u = \sum_m \epsilon_m (n_m - 1/2), \quad (5)$$

with ground state energy  $E_0 = -1/2 \sum_m \epsilon_m$ . The orthogonal matrix  $Q^u$  will have a crucial role in the following to obtain the projection operator.

*Reduced projector  $\mathcal{P}_0$ .* The beauty of Kitaev's solution is to reduce the problem of finding the eigenvalues of a  $2^{2N} \times 2^{2N}$  matrix to the diagonalization of the  $2N \times 2N$  matrices  $A^u$ . However, the final spectrum and eigenstates are in the extended Hilbert space  $\tilde{\mathcal{L}}$ , and a projection  $\mathcal{P}$  to the physical subspace is necessary [1]. The physical states satisfy  $D_i|\Psi\rangle = |\Psi\rangle$  for all the gauge operators  $D_i = b_i^x b_i^y b_i^z c_i$  and the explicit form of  $\mathcal{P}$  is [1]

$$\mathcal{P} = \prod_{i=1}^{2N} \left( \frac{1 + D_i}{2} \right) = \frac{1}{2^{2N}} \sum_{\{i\}} \prod_{i \in \{i\}} D_i, \quad (6)$$

where the summation runs over all possible subsets of indices  $\{i\} \subset \Lambda$ . Within the physical subspace the  $\tilde{\sigma}^{x,y,z}$  operators satisfy the usual algebra of Pauli matrices and therefore  $H$  and  $\tilde{H}$  are equivalent.

Equation (6) is well known, and it is also clear that  $\mathcal{P}$  does not influence the energy and spin-correlation functions of a given eigenstate  $|\Psi\rangle_u \in \tilde{\mathcal{L}}_u$  with a fixed number of fermions (as found with Kitaev's method of solution), if  $\mathcal{P}|\Psi\rangle_u \neq 0$ . However, the fact that not all eigenstates of  $\tilde{H}$  are physical states is generally overlooked. The presence of unphysical eigenstates, for which  $\mathcal{P}|\Psi\rangle_u = 0$ , makes the projection a crucial ingredient to extract the physical properties of  $\tilde{H}$ . In particular, it will become apparent below that the spectra of  $H$  and  $\tilde{H}$  do not coincide.

To establish an explicit formula for  $\mathcal{P}$  we first note that, in the summation appearing in Eq. (6), the two terms corresponding to a subset  $\{i\}$  and its complementary set  $\Lambda \setminus \{i\}$  simply differ by a factor  $\prod_{i=1}^{2N} D_i$ . Therefore, we can factorize  $\mathcal{P}$  as follows

$$\mathcal{P} = \left( \frac{1}{2^{2N-1}} \sum'_{\{i\}} \prod_{i \in \{i\}} D_i \right) \cdot \left( \frac{1 + \prod_{i=1}^{2N} D_i}{2} \right) = S \cdot \mathcal{P}_0, \quad (7)$$

where the prime indicates that the summation in  $\mathcal{S}$  (in the first parenthesis) is restricted to half of all possible subse of indices: if  $\{i\}$  is included  $\Lambda \setminus \{i\}$  is not.

We then consider  $\prod_{i=1}^{2N} D_i$  in the projector  $\mathcal{P}_0$  [the second parenthesis of Eq. (7)]. From the definition of  $D_i$ , it clearly consists of a product of all the  $c_i$  and  $b_i^{x,y,z}$  operators. By applying the anticommutation rules we can pair corresponding  $b_i^{x,y,z}$  operators, and express them in terms of the conserved quantities  $u_{ij}$ . To do this, it is necessary to know the topology of the lattice, from which the correct pairing is determined. We consider here a model defined on a torus with basis vectors  $L_1 \mathbf{e}_1$  and  $L_2 \mathbf{e}_2 + M \mathbf{e}_1$ , as illustrated in Fig. 1. This represents the most general choice of periodic boundary conditions and  $N = L_1 L_2$ . It is also necessary to fix the correspondence between  $i = 1, \dots, 2N$  and lattice sites. We fix the labeling such that  $i = 1, \dots, N$  and  $i + N$  are respectively site  $A$  and  $B$  of the same  $z$ -dimer, see Fig. 1. After pairing the  $b_i^{x,y,z}$  operators we find that the remaining product of all  $c_i$  operators can be simply expressed in terms of the eigenmodes:

$$c_1 \dots c_{2N} = \det(Q^u) b'_1 b''_1 \dots b'_N b''_N. \quad (8)$$

Finally,  $\mathcal{P}_0$  can be written as follows:

$$2\mathcal{P}_0 = 1 + (-1)^\theta \det(Q^u) \prod_{\langle i,j \rangle} u_{ij} \hat{\pi}, \quad (9)$$

where  $\theta = L_1 + L_2 + N(N+1)/2 + M(L_1 - M)$  and  $\hat{\pi} = \prod_{m=1}^N (1 - 2n_m)$  is the parity operator with eigenvalues  $+1(-1)$  if the total number of fermions is even (odd).

The form of Eq. (9) is extremely convenient. For a given configuration of  $u_{ij} = \pm 1$ , the matrix  $Q^u$  is orthogonal and  $\det(Q^u) = \pm 1$ . An eigenstate  $|\Psi\rangle_u \in \tilde{\mathcal{L}}_u$  in the Kitaev's solution is identified with the occupation numbers and  $(2n_m - 1) = \pm 1$ . Therefore, Eq. (9) shows that  $\mathcal{P}_0$  is either 0 or 1 on the eigenstate  $|\Psi\rangle_u$ . In the former case, the state is clearly unphysical. In the second case,  $\mathcal{P}|\Psi\rangle_u = \mathcal{S}|\Psi\rangle_u \neq 0$  since, as seen in Eq. (7), the  $2^{2N-1}$  terms of  $\mathcal{S}$  all correspond to different configurations of  $u_{ij}$ . In conclusion, Eq. (9) determines immediately if  $|\Psi\rangle_u$  has some overlap with the physical subspace (in which case  $|\Psi\rangle_u$  is called physical state) or lies completely outside of it.

A first immediate consequence of Eq. (9) is that only half of the eigenstates in the extended Hilbert space are physical. Indeed the product  $p_u = (-1)^\theta \det(Q^u) \prod_{\langle i,j \rangle} u_{ij}$  is fixed by the configuration  $u$ . When such product is  $+1$ , the physical states are the vacuum state of the extended model ( $n_m = 0$ ) and all excited states with an *even* number of fermions, while the excitations with an *odd* number are unphysical. When the product is  $-1$ , the states with an odd number of fermions are physical. It is consequently clear that the crucial quantity which determines if a state is unphysical is the parity of fermions  $\hat{\pi}$ . An eigenstate  $|\Psi\rangle_u$  lies completely

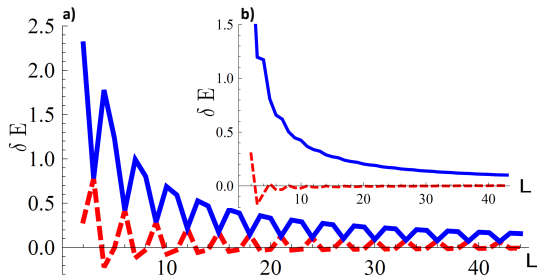


FIG. 2: Physical (solid line) and unphysical (dashed line) finite size corrections to the thermodynamic energy of a vortex-free configuration  $u_{ij} = 1$ . We used  $J_x = J_y = J_z = 1$  and  $L_1 = L_2 = L$ . The main plot a) and inset b) refer to  $M = 0$  and  $M = 1$ , respectively.

outside of the physical subspace if  $\hat{\pi}|\Psi\rangle_u = -p_u|\Psi\rangle_u$ . These conclusions are consistent with a simpler counting argument: the extended Hilbert space has dimension  $2^{4N}$  but the eigenstates are highly degenerate, due to the presence of  $2^{2N}$  gauge transformations of the form  $\prod_{i \in \{i\}} D_i$ . However, as noted above, the two gauge transformations corresponding to  $\{i\}$  or  $\Lambda \setminus \{i\}$  differ at most by a sign, when applied to a given eigenstate  $|\Psi\rangle_u$ . For this reason the degeneracy is only  $2^{2N-1}$  and there are in general  $2 \times 2^{2N}$  distinct eigenvalues, instead of  $2^{2N}$  as in the original model.

*Vortex-free sector.* The crucial quantity in Eq. (9) is  $\det(Q^u)$ , which we now explicitly evaluate in the vortex-free sector with  $u_{ij} = 1$ . We can proceed as in [1] by making use of the Fourier transform  $a_{\mathbf{q}\lambda} = (1/\sqrt{2N}) \sum_s e^{-i\mathbf{q}\cdot\mathbf{r}_s} c_{s\lambda}$  on the lattice. Here we have relabeled  $c_i \equiv c_{s\lambda}$  where  $\mathbf{r}_s = s_1\mathbf{e}_1 + s_2\mathbf{e}_2$  indicates the position of a  $z$ -dimer and  $\lambda = A, B$  the sublattice (see Fig. 1). The  $N$  possible values of  $\mathbf{q}$  are fixed by the periodicity of the lattice and we say that  $\mathbf{q} \in \Omega$  if  $\pm\mathbf{q}$  are the same (up to reciprocal lattice vectors).  $\Omega$  contains at most 4 wavevectors, depending on  $L_{1,2}$  and  $M$ , and always contains  $\mathbf{0}$ . The remaining wavevectors can be partitioned in a way that  $\pm\mathbf{q}$  always belong to two distinct sets  $\Omega_{\pm}$ . We define new Majorana modes as  $\gamma_{\mathbf{q}}^{\lambda} = \sqrt{2}a_{\mathbf{q}\lambda}$  for  $\mathbf{q} \in \Omega$  and

$$\gamma_{\mathbf{q},1}^{\lambda} = a_{\mathbf{q}\lambda} + a_{-\mathbf{q}\lambda}, \quad \gamma_{\mathbf{q},2}^{\lambda} = i(a_{\mathbf{q}\lambda} - a_{-\mathbf{q}\lambda}), \quad (10)$$

for  $\mathbf{q} \in \Omega_+$ . This canonical transformation of the  $c_{s\lambda}$  has two identical blocks labeled by  $\lambda = A, B$ , and the determinant is simply 1.

The Hamiltonian, rewritten in terms of the new Majorana modes, is diagonal in  $\mathbf{q}$  and its coefficients are given by  $f(\mathbf{q}) = 2(J_x e^{i\mathbf{q}\cdot\mathbf{e}_1} + J_y e^{i\mathbf{q}\cdot\mathbf{e}_2} + J_z)$  and its complex conjugate. A further diagonalization with respect to the index  $\alpha$  of  $\gamma_{\mathbf{q},\alpha}^{\lambda}$  is achieved with the rotation

$$\begin{pmatrix} \tilde{\gamma}_{\mathbf{q},1}^B \\ \tilde{\gamma}_{\mathbf{q},2}^B \end{pmatrix} = \begin{pmatrix} \cos(\phi_{\mathbf{q}}) & \sin(\phi_{\mathbf{q}}) \\ -\sin(\phi_{\mathbf{q}}) & \cos(\phi_{\mathbf{q}}) \end{pmatrix} \begin{pmatrix} \gamma_{\mathbf{q},1}^B \\ \gamma_{\mathbf{q},2}^B \end{pmatrix}, \quad (11)$$

where  $\phi_{\mathbf{q}}$  is the phase of  $f(\mathbf{q})$ , i.e.,  $f(\mathbf{q}) = |f(\mathbf{q})|e^{i\phi_{\mathbf{q}}}$ . This transformation has again determinant 1 and brings  $\tilde{H}_u$  to the form

$$\tilde{H}_u = \frac{i}{2} \left( \sum_{\mathbf{q} \in \Omega_+} |f(\mathbf{q})| \sum_{\alpha=1,2} \gamma_{\mathbf{q},\alpha}^A \tilde{\gamma}_{\mathbf{q},\alpha}^B + \sum_{\mathbf{q} \in \Omega} f(\mathbf{q}) \gamma_{\mathbf{q}}^A \gamma_{\mathbf{q}}^B \right). \quad (12)$$

Finally, as discussed below Eq. (4),  $Q^u$  brings the Hamiltonian to the form  $\tilde{H}_u = \frac{i}{2} \sum_{\mathbf{q}} \epsilon(\mathbf{q}) b'_{\mathbf{q}} b''_{\mathbf{q}}$  with  $\epsilon(\mathbf{q}) \geq 0$ . This can be achieved in Eq. (12) by relabeling the Majorana operators. If  $\mathbf{q} \in \Omega_+$ :  $b'_{\mathbf{q}} = \gamma_{\mathbf{q},1}^A$ ,  $b''_{\mathbf{q}} = \tilde{\gamma}_{\mathbf{q},1}^B$ ,  $b'_{-\mathbf{q}} = \gamma_{\mathbf{q},2}^A$ ,  $b''_{-\mathbf{q}} = \tilde{\gamma}_{\mathbf{q},2}^B$ . If  $\mathbf{q} \in \Omega$  and  $f(\mathbf{q}) \geq 0 (< 0)$ :  $b'_{\mathbf{q}} = \gamma_{\mathbf{q}}^{A(B)}$ ,  $b''_{\mathbf{q}} = \gamma_{\mathbf{q}}^{B(A)}$ . The determinant of this last transformation coincides with  $\det(Q^u)$  and is given by

$$\det(Q^u) = (-1)^{\chi + N(N-1)/2} \quad \text{for } u_{ij} = 1, \quad (13)$$

where  $\chi$  is the number of reciprocal lattice vectors  $\mathbf{q} \in \Omega$  such that  $f(\mathbf{q}) < 0$ . Notice that  $\chi$  depends in a non-trivial way on the boundary conditions  $L_{1,2}, M$ , and the couplings  $J_{x,y,z}$ . Nevertheless, for a given choice of the model, it can be easily computed. For an arbitrary  $u$  configuration, Fourier transformation cannot be used to calculate  $\det(Q^u)$  analytically. However,  $\det(Q^u)$  can be determined numerically with little computational effort.

*Numerical applications.* We now consider some numerical applications of Eq. (9). Following [1], we plot in Fig. 2 the finite size correction  $\delta E = E_0(N) - \epsilon_0 N$  to the ground-state energy with  $u_{ij} = 1$ ,  $J_x = J_y = J_z = 1$ , a square lattice ( $L_1 = L_2 = L$ ), and two different boundary conditions ( $M = 0, 1$ ). The energy per unit cell is  $\epsilon_0 \simeq -1.5746$  in the thermodynamic limit [1]. The solid line represents our result. The original result calculated in [1] is also reproduced in Fig. 2 (dashed lines) and evidently refers to the unphysical energy, which always underestimates the correct result. The physical and unphysical energies are always distinct, unless  $\epsilon_m = 0$  for some fermion mode. This difference clearly shows that, for finite size systems, it is not sufficient to calculate the energy of the system in the extended space but our projection protocol must be applied to take advantage of all the power of Kitaev's exact mapping. On the other hand, the difference between physical and unphysical energy approaches zero at large system size.

We consider next the energy to create vortices in the system. These are present on hexagonal cells for which the product of the six  $u_{ij}$  is  $-1$ . As an interesting example we study a configuration with two adjacent vortices, obtained by setting  $u_{ij} = -1$  for a single link. We assume again  $J_x = J_y = J_z = 1$  but consider here the same lattice of the toric code [4]:  $L_1 = 2L$  and  $L_2 = M = L$ . In Fig. 3 we plot the excitation energy per vortex  $\Delta E = \frac{1}{2}[E_2(L) - E_0(L)]$ , where  $E_{0,2}(L)$  are the ground state energies of the vortex-free and two-vortex configuration, respectively. Since the vortex state is not

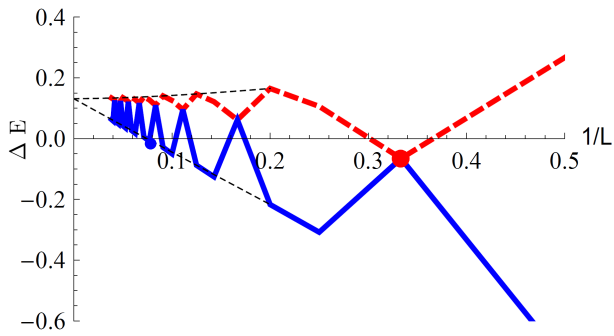


FIG. 3: Physical (thick solid line) and unphysical (thick dashed line) excitation energy of a pair of adjacent vortices. We used  $J_x = J_y = J_z = 1$ ,  $L_1 = 2L$ , and  $L_2 = M = L$ . Thin dashed lines extrapolate to the thermodynamic limit. The dots at  $L = 3$  (unphysical) and  $L = 13$  (physical) represent the largest system sizes with negative excitation energy.

translationally invariant, we obtain the energy spectrum numerically. This can be done efficiently, since it only involves  $2N \times 2N$  matrices. In Fig. 3 we show physical excitation energies up to  $L = 26$  (corresponding to 2704 physical spins), obtained with a standard tabletop computer and high level language routines (MATLAB). We have checked that for the lowest possible system size the spectrum obtained with this method is in agreement with direct diagonalization of the physical model. However, direct diagonalization is limited to systems with only a few tens of spins, by making use of very intensive parallel computing numerical routines [9, 11].

Similarly to Fig. 2, physical and unphysical results are generally different. They become equal only in the thermodynamic limit when  $\Delta E(\infty) \simeq 0.132$ , independently of the boundary conditions (see [1] for a different choice). We find here that the physical excitation energy is generally lower than the unphysical one and finite size corrections are very important:  $\Delta E$  shows pronounced oscillations, with an amplitude which is of the same order of magnitude of  $\Delta E(\infty)$ , for up to a few thousand spins. Remarkably, such oscillations result in negative excitation energies of the vortex pair up to 676 spins (instead of 36, in the extended space).

From our projection formula Eq. (9) it is also immediate to understand why the energies of Figs. 2 and 3 agree with the unphysical values at large system size. In each sector  $u$ , the physical and unphysical states with lowest energy only differ by a single fermion (the one with lowest energy  $\epsilon_m$ ). Whenever the model is gapless, such difference is zero in the thermodynamic limit, and is of order  $\sim 1/L$  for finite size. However, only eigenstates  $|\Psi\rangle_u$  satisfying  $\hat{\pi}|\Psi\rangle_u = +p_u|\Psi\rangle_u$  have overlap with the physical subspace and lead to a correct description of the model.

Similar considerations on the relevance of the projection operator apply to the spin correlation functions  $S_{ij}^{\alpha\beta}(t) = \langle \sigma_i^\alpha(t) \sigma_j^\beta(0) \rangle$ , whose exact properties were dis-

cussed in [12]. By using Kitaev's exact mapping it is possible to address large lattices and it is convenient to compute  $S_{ij}^{\alpha\beta}(t)$  with unprojected eigenstates  $|\Psi\rangle_u$  [12]. This is possible thanks to the fact that the spin operators  $\tilde{\sigma}_i^\alpha$  are gauge-invariant. However, one should again make sure that only states with  $\mathcal{P}|\psi\rangle_u \neq 0$  are included. We have calculated  $S_{ij}^{\alpha\beta}(0)$  and found finite-size deviations from the unprojected results, similar to Figs. 2 and 3. More generally it is obvious from our discussion that all dynamic and thermodynamic quantities derived from  $H$  (for example, the partition function), depend on the physical spectrum and eigenstates and thus differ from those of the unprojected model  $\tilde{H}$ .

*Conclusion.* We have obtained here an explicit form of the projection operator which allows us to extract the physical properties of the honeycomb model for large lattices. Our method reveals that the numerical solution of the model without projection [1, 15] is not accurate. Our work is generally relevant to spin models to which the Kitaev's method of solution applies, like the honeycomb model perturbed by a weak magnetic field [1, 9] or interacting with cavity modes [6], and a three dimensional Kitaev model recently proposed in Ref. [14]. The case of open boundary conditions can also be simply obtained considering an extension of Eq. (1) with site-dependent couplings  $J_{\alpha ij} \rightarrow J_{ij}$  (and  $J_{ij} = 0$  on the boundary).

*Acknowledgments.* We thank David P. DiVincenzo for inspiring suggestions. We also acknowledge discussions with Suhas Gangadharaiyah, Diego Rainis, Beat Röthlisberger, and Luka Trifunovic. This work was supported by the Swiss NSF, NCCR Nanoscience, NCCR QSIT, DARPA QuEST, and the EU project SOLID. SC acknowledges support from CIFAR.

- 
- [1] A. Kitaev, Ann. Phys. **321**, 2 (2006).
  - [2] G. Jackeli and G. Khaliullin, Phys. Rev. Lett. **102**, 017205 (2009).
  - [3] K. S. Tikhonov, M. V. Feigel'man, and A. Yu. Kitaev, Phys. Rev. Lett. **106**, 067203 (2011).
  - [4] A. Kitaev, Ann. Phys. **303**, 2 (2003).
  - [5] S. Chesi, B. Röthlisberger, and D. Loss, Phys. Rev. A **82**, 022305 (2010).
  - [6] F. L. Pedrocchi, S. Chesi, and D. Loss, Phys. Rev. B **83**, 115415 (2011).
  - [7] L.-M. Duan, E. Demler, and M. D. Lukin, Phys. Rev. Lett. **91**, 090402 (2003).
  - [8] J. Q. You, X.-F. Shi, X. Hu, and F. Nori, Phys. Rev. B **81**, 014505 (2010).
  - [9] V. Lahtinen, G. Kells, A. Carollo, T. Stitt, J. Vala, and J. K. Pachos, Ann. Phys. **323**, 2286 (2008).
  - [10] G. Kells, N. Moran, and J. Vala, J. Stat. Mech. (2009) P03006.
  - [11] J. Chaloupka, G. Jackeli, and G. Khaliullin, Phys. Rev. Lett. **105**, 027204 (2010).
  - [12] G. Baskaran, S. Mandal, and R. Shankar, Phys. Rev. Lett **98**, 247201 (2007).

- [13] G. Kells, A. T. Bolukbasi, V. Lahtinen, J. K. Slingerland, J. K. Pachos, and J. Vala, Phys. Rev. Lett. **101**, 240404 (2008).
- [14] S. Mandal and N. Surendran, Phys. Rev. B **79**, 024426 (2009).
- [15] H. Xu and J. M. Taylor, arXiv:1104.0024 (2011).
- [16] K. I. Kugel' and D. I. Khomskii, Sov. Phys.-Usp. **25**, 231 (1982).
- [17] Whenever we specify the values of  $u_{ij}$ , we assume that  $i$  is in the A sublattice (see Fig. 1). Otherwise,  $u_{ij} = -u_{ji}$ .